HOM ABSORBERS FOR ERL CRYOMODULES AT BNL*

H. Hahn#, I. Ben-Zvi, L. Hammons, W. Xu,
Brookhaven National Laboratory, Upton, NY, U.S.A.

Abstract

The physics needs and technical requirements for several future accelerator projects at the Relativistic Heavy Ion Collider (RHIC) all involve electron Energy Recovery Linacs (ERL). The required high-current, high-charge operating parameters make effective higher-order-mode (HOM) damping mandatory and the development of HOM dampers for a prototypical five-cell cavity is actively pursued. An experimental five-cell niobium cavity with ferrite dampers has been constructed, and effective HOM damping has been demonstrated at room- and superconducting (SC) temperatures. A novel type of ferrite damper around a ceramic break has been developed for the ERL electron gun and prototype tests are also reported. Contemplated future projects are based on assembling a chain of superconducting cavities in a common cryomodule with the dampers placed in the cold space between the cavities, imposing severe longitudinal space constraints. Various damper configurations have been studied by placing them between two five-cell copper cavities. Measured and simulated copper cavity results, external *Q*-values of possible dampers and fundamental mode losses are presented.

INTRODUCTION

The development of (HOM) dampers is performed at this laboratory in support of three programs directed at (1) an experimental 703 MHz Energy Recovery Linac (ERL) facility [1]; (2) the superconducting (SC) cavities for a medium energy, polarized electron-ion collider (MeRHIC) as a stage toward the realization of a 20 MeV electron-ion facility in the Relativistic Heavy Ion Collider (eRHIC) [2]; and (3) steps toward a proof-of-principle experiments for coherent electron cooling [3]. HOM damping is crucial to the performance of these projects in view of their high-current, high-brightness, and high-charge requirements.

The ERL facility is comprised of a five-cell SC Linac plus a half-cell SC photo-injector RF electron gun [4], both operating at 703.75 MHz. The facility is designed for either a high-current mode of operation up to 0.5 A at 703.75 MHz or a high-bunch-charge mode of 5 nC at 10 MHz bunch frequency. The facility will be assembled with a highly flexible lattice covering a vast operational parameter space to serve as a test bed for the technologies and concepts necessary for future projects including the MeRHIC. HOM damping is accomplished by ferrite absorbers attached to either side of the cavity.

*Work supported by Brookhaven Science Associates, LLC under Contract No. DE-AC02-98CH10886 with the U.S. DOE.
#hahnh@bnl.gov

At present, the SC 5-cell cavity string has been installed, and several cold tests have been performed with the damping of dipole modes summarized in Table 1 [5].

Table 1 : Dipole modes of SC ERL cavity

f_{MWS} [MHz]	$f_{SC\ (4\ K)}$ [MHz]	R/Q_{MWS} [Ω]	Q_{Cu+Fe}	Q_{SC} (4K)	$R_{\perp}$ [kΩ/m]
803.4	808.5	0.13	588	1031	2.25
808.4	--	1.12	150	--	--
816.1	--	0.73	136	--	--
827.0	826.0	0.22	265	426	1.63
849.5	849.8	11.84	493	147	30.88
872.6	--	49.33	379	--	--
888.1	--	42.01	163	--	--
895.0	--	22.78	201	--	--
926.2	--	6.66	104	--	--
940.7	--	8.58	79	--	--
956.1	960.0	0.05	40,370	46,000	45.96
962.2	966.0	2.65	6,410	5126	273.12
973.7	978.6	8.07	2,132	593	97.40
989.8	995.9	2.39	1,644	296	14.63

The MeRHIC will employ five-cell SC cavities based on the type being used in the ERL facility but upgraded depending on the experience gained. The physics program requires 5 nC bunches in the 46 mA electron current to be accelerated to 4 GeV for collision with 250 GeV protons in RHIC. A key consideration in this project is that the design of the cryomodules and accompanying structures be highly compact and modular. The present concept sees the electron LINAC to be a chain of sections as shown in Fig. 1, each employing six five-cell cavity cryo-modules. The HOM dampers will be placed into the cold section between two cavities. The primary focus in the present study is on using capacitive dampers which is simulated by placing the HOM damper structures between to copper cavities as shown in Fig. 2.

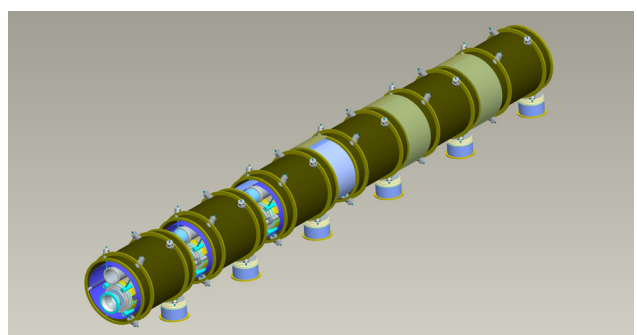

Figure 1: A MeRHIC linac section with 6 cryo-modules.

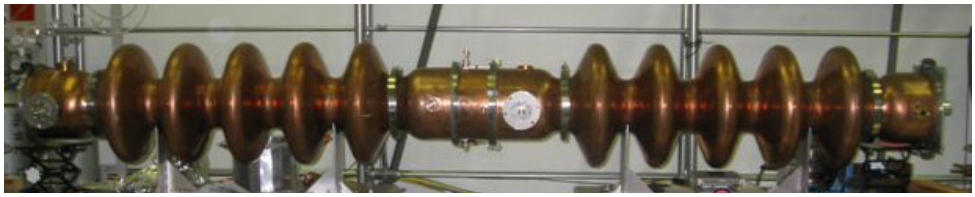

Figure 2: The HOM damper ring with capacitive probes between two copper cavities.

THE CAVITY STRING MODEL

The summary goal of the present damper studies is the creation of a list with best estimates for the shunt impedance of dipole cavity resonances. The estimates are based on the measured *Q*-external and the R/Q from computer simulation. The measurement of the external *Q* follows from the difference of the unloaded and loaded *Q*. To be valid for the linac string both tasks require a model beyond the conventional single cavity. The string is sufficiently replicated by the two cavity arrangement in Fig. 2 and by the simulation by the Microwave Studio (MWS) model in Fig. 3. Quoting the effectiveness of a damper and consistency of results mandates that both structure ends are shorted. The MWS simulation results for the lowest two dipole pass bands are given in Table 2. The longitudinal integral is done off-axis at $a = 1$ cm and interpreted as

$$(R/Q)_{\perp} = (R/Q)_{\parallel} / ka^2 .$$

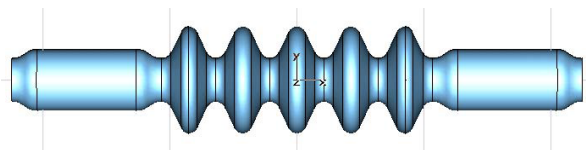

Figure 3: MWS cavity model.

Table 2 : Simulation of dipole resonances

f [MHz]	$R/Q_{\parallel}$ [Ω]	$R/Q_{\perp}$ [Ω]	$R/Q_{\perp}$ [Ω/m]	Mode Type
775.69	0.003503	0.13	2.16	B
775.71	0.005878	0.22	3.62	B
808.82	0.003477	0.12	2.05	C
826.17	0.02781	0.93	16.08	C
849.08	0.1748	5.53	98.31	C
870.13	1.2041	36.27	660.85	C
883.26	1.7304	50.58	935.58	C
890.06	0.9097	26.19	488.09	C
931.04	0.8552	22.50	438.65	E
931.06	0.2273	5.98	116.59	E
959.43	0.001826	0.05	0.91	C
965.68	0.1062	2.60	52.52	C
977.63	0.3045	7.27	148.74	C
994.38	0.09844	2.27	47.28	C
1064.83	0.008471	0.17	3.80	B
1065.73	0.05258	1.06	23.56	B
1199.06	0.03856	0.61	15.36	E

Note the larger number of resonances actually found compared to the expected ones in a free-standing single cavity, identified as "C" in the table. The additional resonances are pure beam tube resonances, "B", or are located mainly in the end cells, "E". The design was based on the concept that a large beam tube aperture, here 24 cm, allows exit of the HOMs from the cavity to the damper, which in fact is confirmed by the measurements discussed below. The beam tube resonances with Fig. 4 as example are locally damped, whereas the end cell resonances, e. g. Fig. 5, may not be strongly connected to the dampers.

An example of a quasi-trapped resonance is found at ~959 MHz which has the fields concentrated in the center cell and minimal connection to any damper in the adjacent beam tube. The longitudinal and transverse electric and transverse magnetic field components shown in Fig. 6 are concentrated within the nominal cavity length of 2 × 63 cm and have essentially no extension into the inter-cavity connection.

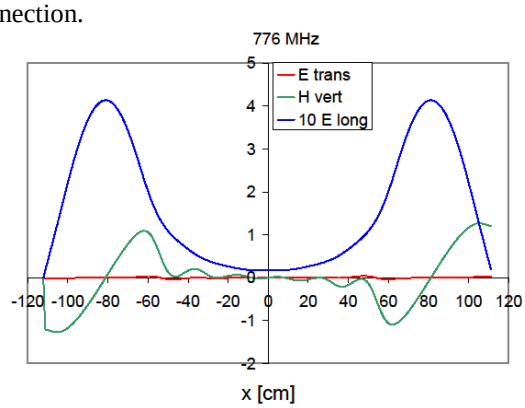

Figure 4: Fields in beam tube at 776 MHz.

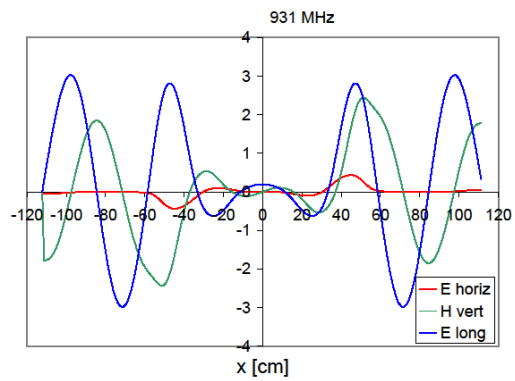

Figure 5: Fields in end cell at 931 MHz.

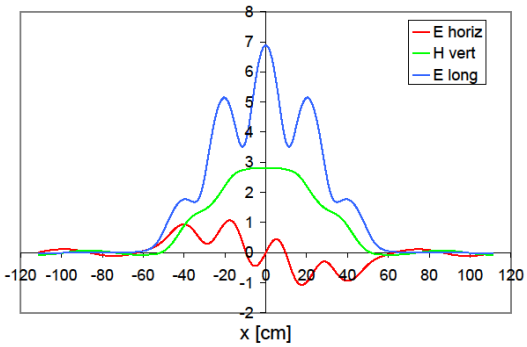

Figure 6: Fields in the cavity at 959 MHz resonance.

Another effect of large beam tubes is the coupling and the resulting frequency shift and splitting seen in Fig. 7 of the un-damped HOMs in neighboring cavities. Note however that there is essentially no coupling between the two cavities at the fundamental.

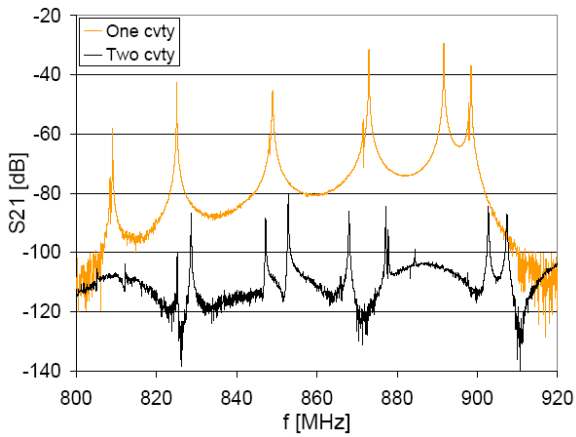

Figure 7: Frequency splitting of HOMs.

CAPACITIVE DAMPERS

The HOM dampers are attached to a spacer ring and placed in the cold section between two cavities of the present type as shown in Fig. 8. Since the ring is also between Fundamental Power Coupler (FPC) and RF pickup probe (PU), damping of the fundamental power and cross coupling FPC to PU must be considered in addition to the HOM damping. The length of the damper ring and its location with respect to the cavities is a critical design parameter, and is selected for strong damping together with the shortest overall length and minimum coupling to the fundamental.

Several damper geometries based on inductive, capacitive, and ferrite have been studied. The ring with capacitive probes, 2 inch diameter disk, 1 inch long stem is shown in Fig. 9. Its simulated and measured frequencies and measured Q-external are listed in Table 3. The capacitive probes are centered in the ring which places them at 7 inch from the left and 8.5 inch from the right cavity, which explains the difference in the Q-values of the split cavity resonances. The column indicated by (wo) is obtained with dampers of equal length but removed disks, pointing to the 2-inch dia., 1-inch long capacitive probes as appropriate dampers. It can be expected that placing damper rings at both cavity ends will half the *Q*-values.

The fields of the HOMs in the beam tube are stationary even though they are above cutoff and the axial location of the probes determines the coupling strength. Measurements with staggered placements of the probes were performed and the results listed in Table 4, indicating improved damping. Staggered dampers with three probes at 2, 6, 10 and at 4, 8, 12 o'clock seems optimum.

Figure 8: Connecting tube with damper ring.

Table 3: Simulated and measured frequencies and their measured *Q*-external

f MWS [MHz]	f Data [MHz]	Q_0	Q_L	Q_X	Q_X (wo)
808.8	806.3	11,370	9940	79,033	311,822
	814.3	7090	5310	21,151	125,194
826.2	825.1	17,050	4190	5555	42,889
	828.6	9450	2490	3381	24,249
849.1	847.1	1,440	3610	4936	44,270
	852.8	10,980	1680	1983	17,521
870.1	867.9	10,520	2770	3760	35,593
883.3	877.2	13,570	2603	3221	38,448
890.1	884.3	7990	3290	5593	50,046
959.4	958.2	35,390	29,460	175,816	4,283,410
	958.7	34,900	2,880	138,606	5,501,509
965.7	965.6	13,950	17,760	65,027	26,151
977.6	976.7	19,370	3440	4183	124,384
	978.0	23,400	13,000	29,250	165,414
994.3	994.5	1340	1100	1199	8335
	996.8	15,090	4840	7125	71,821

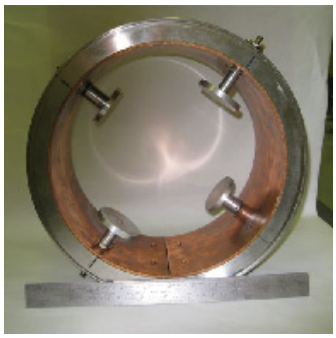

Figure 9: Axially staggered capacitive probes.

Table 4: Frequencies and *Q*-values with staggered dampers

f [MHz]	Q_0	Q_L	Q_X
808.0	5810	3260	7428
808.6	4260	2520	6170
819.3	5660	4460	21,036
825.0	17,920	100	101
833.0	9740	4970	10,148
846.2	12,440	1540	1758
854.6	11,310	3280	4620
865.8	3420	10	10
877.0	12,180	1400	1582
883.2	6300	2040	3017
958.7	33,040	22,790	73,462
965.5	28,650	4830	2809
976.9	13,050	100	101
877.8	15,670	1850	2098
995.0	8660	3880	7029
996.4	8770	2240	3008

The *Q*-external at the fundamental mode attributable to the four probes in the ring and its variation with their geometry and location was measured and is shown in Fig. 10. The HOM damping in Table 3 is achieved with an external cavity *Q* of only ~ 1×10^8 but higher values are limited by the required damping. The capacitive ring adds 5 inch to the cavity length and reducing the fundamental load by an order of magnitude would require about 3 inch additional length.

Fundamental cross coupling between FPC and dampers was found to be ~3×10^{-3}. Suppression of fundamental losses requires added length or a filter of the type shown in Fig. 11. The filter shown was designed by Sekutowicz for a prototype electron gun cavity, but the separation between the fundamental frequency and the HOM high-pass is not steep enough and a notch filter would have to be developed [6].

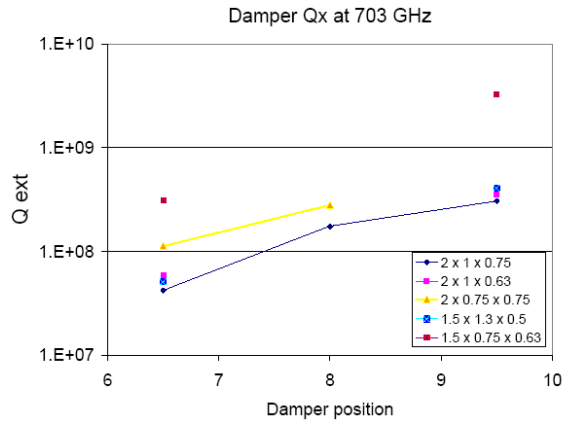

Figure 10: Q-external versus damper position and probe size (disk diameter × stem length × diameter).

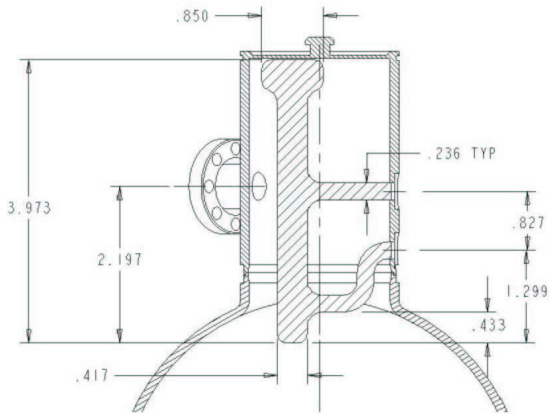

Figure 11: HOM damper with built in fundamental filter (dimensions in inch).

FERRITE DAMPERS

The prototype ferrite absorber in Fig. 12 which remained from the damping studies for the ERL was placed between the Copper cavities to replace the capacitive damper ring as seen in Fig. 13. The measurements with the ERL ferrite damper produced the strongest HOM damping so far. The changes of the resonance frequencies and the qualitative pictorial of the damping is plotted in Fig. 14 against the un-damped two-cavity results. The ferrite damped Q-values listed in Table 5 are sufficiently low to be treated as the Q-external values in estimating the shunt impedance.

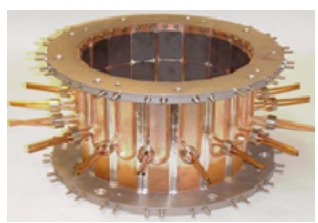

Figure 12: Prototype ferrite HOM load.

Figure 13: Ferrite damper between the cavities.

Table 5: Ferrite damped HOM resonances

f [MHz]	Q_L	f [MHz]	Q_L
808.4	4690	958.1	13,210
809.0	4380	958.6	13,390
825.3	1480	964.7	1950
849.1	910	974.0	580
858.2	130	985.9	460
873.1	580	1001.3	790
879.3	410		
892.0	630		
897.9	2110		

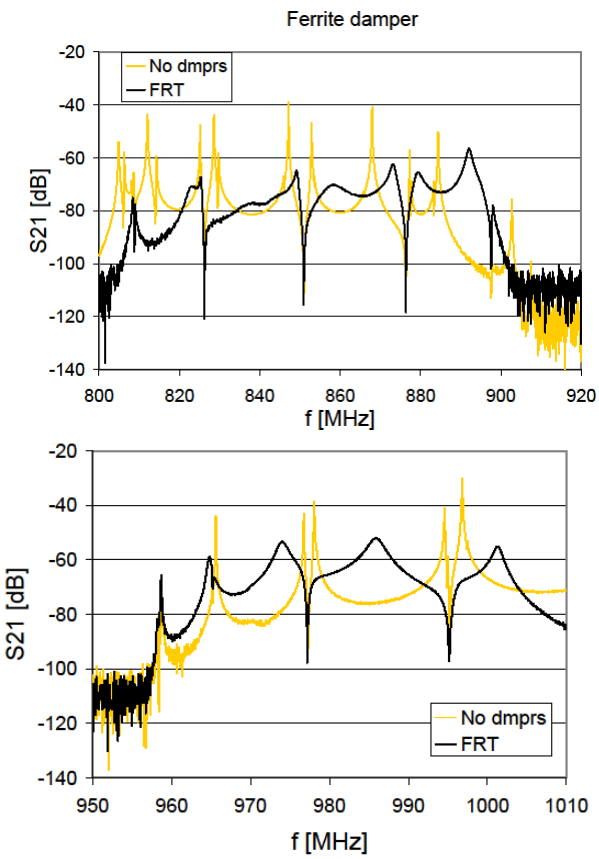

Figure 14: Ferrite damping of the HOMs versus the un-damped two coupled cavities.

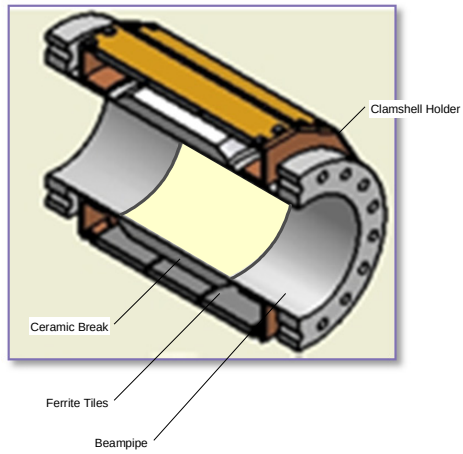

Figure 15: Ferrite HOM damper with ceramic break.

FERRITE DAMPER OVER CERAMIC BREAK

The associated fundamental damping of the prototype ERL ferrite has not yet been determined, but is likely to be unacceptable for space reasons. A novel damper configuration separating the ferrite from the beam vacuum by the insertion of a ceramic beam tube, 10 cm i.d., and allowing cooling at intermediate temperatures is a promising compromise between on one hand strong HOM damping and economic cooling on the other hand. The ceramic (alumina) break must be coated with a thin film of titanium-enhanced stainless steel with an end to end resistance of ~10 to 100 MΩ to prevent static charge accumulation. The multi-layer structure was analyzed and confirmed the damping properties [8]. A ferrite HOM damper with ceramic break is constructed for the ERL electron gun [4] and will provide the basis for further development.

REFERENCES

[1] I. Ben-Zvi, ERL Prototype at BNL, these Proc.
[2] V. Ptitsyn, et al., 2009 Particle Accelerator Conference (Vancouver, Canada, 2009).
[3] V. N. Litvinenko and Y. S. Derbenev, Phys. Rev. Letters 102 (11) (2009).
[4] R. Calaga, et al., Physica C-441 (1-2), 159-172 (2006).
[5] H. Hahn, E. M. Choi, and L. Hammons, Phys. Rev. S T. Accel. Beams, 12 (2) (2009).
[6] Y Zhao and H. Hahn, HOM measurement and simulation, Internal Report C-A/AP/61 (BNL, 2004).
[7] L. Hammons and H. Hahn, HOM Absorber development for SC BNL ERL, Proc. Cornell ERL09.
[8] H. Hahn, Matrix solution to longitudinal impedance of multi-layer circular structures, Internal Report C-A/AP/336 (BNL, 2008).